Pharmacology & Therapeutics 131 (2011) 359–368

Contents lists available at ScienceDirect

Pharmacology & Therapeutics

journal homepage: www.elsevier.com/locate/pharmthera

Associate Editor: Jeffrey Fedan

Noninvasive pulmonary function screening in spontaneously breathing rodents: An engineering systems perspective

Jeffrey S. Reynolds *, David G. Frazer

Pathology and Physiology Research Branch, National Institute for Occupational Safety and Health, Centers for Disease Control and Prevention, 1095 Willowdale Road, Morgantown, WV 26505, USA

ARTICLE INFO

Keywords:
Whole-body plethysmograph
Pulmonary function tests
Respiratory function tests
Lung models
Airway resistance

ABSTRACT

Noninvasive pulmonary function measurements made on rodents are commonly used for studies where quick, relatively easy end-points are required. These types of measurements are of particular advantage for studies where large numbers of animals are involved. Using tests that are simple to administer generally translates to more efficient and more accurate data collection. Noninvasive measurements result in less stress placed on the animal and allow repeated testing of the same animals at multiple time points. This review focuses on several noninvasive methods that have been developed for pulmonary function screening, which are analyzed from an engineering systems perspective. An analog model of the respiratory system of a conscious, freely respiring animal is presented in terms of an equivalent electrical circuit. This model is used as a basis to demonstrate the relationship between pulmonary parameters derived from circuit analysis.

Published by Elsevier Inc.

Contents

1. Introduction

Many methods have been developed for measuring pulmonary function in small laboratory rodents. The subset of these methods that are noninvasive in nature provides important screening tools for pharmacological and toxicological studies. There are many instances where relatively quick and easy pulmonary measurements are required. This includes cases involving large numbers of animals, where there is not time to perform more complicated or invasive testing. Noninvasive methods are also beneficial for longitudinal studies where the same animals can be measured repeatedly over the time-course of a treatment or exposure. There are also many cases where the measurements provided by these screening tools are not the primary endpoints. However, these measurements can still provide valuable supporting data for studies involving more invasive and/or destructive testing following some pharmacological or toxicological exposure or intervention.

Several groups have reviewed the spectrum of noninvasive and invasive testing methods commonly used. Bates and Irvin (2003) discuss several pulmonary function measurement types, both

* Corresponding author at: Pathology and Physiology Research Branch, National Institute for Occupational Safety and Health, 1095 Willowdale Road, Morgantown, WV 26505, USA. Tel.: +304 285 6238; fax: +304 285 6265.
E-mail addresses: jreynolds@cdc.gov (J.S. Reynolds), dfrazer@cdc.gov (D.G. Frazer).

0163-7258/$ – see front matter. Published by Elsevier Inc.
doi:10.1016/j.pharmthera.2011.05.003

noninvasive and invasive, and their respective tradeoffs between natural conditions and measurement precision. Glaab et al. (2005) compared a noninvasive measurement (mid-expiratory flow) with invasive measures of lung resistance and dynamic lung compliance in an allergic model of airway responsiveness in mice. Hoymann (2006) focused on these same measures while also reviewing several other commonly used pulmonary function measurements, both noninvasive and invasive. Similarly, Glaab et al. (2007) reviewed several noninvasive and invasive systems used to assess pulmonary function in mice.

This review is focused on screening methods that are noninvasive in nature, including some recently developed techniques that have not been reviewed previously. Additionally, these techniques are presented using an engineering systems approach. This type of approach, including the use of electric circuit analog models and the Laplace transform is certainly not novel in regard to the respiratory system. We believe that this approach not only simplifies the analysis, but also promotes a more intuitive understanding of the relationships between the different screening methods and the parameters they measure.

2. Overview

A simple model of the respiratory system is shown in Fig. 1. A pressure at the body surface, $P_{bs}(t)$, produces a flow of gas, $I_t(t)$, that is forced through the respiratory system, *RS*. As this flow moves through the system it is filtered by the mechanical properties of *RS*, resulting in a flow, $I_a(t)$, and a pressure, $P_{ao}(t)$, at the airway opening. Here, $I_a(t)$ is defined as the volumetric flow at body temperature and saturated humidity.

A common representation of *RS* is the respiratory model (DuBois et al., 1956) shown in Fig. 2.

In this model, P_{alv} is the alveolar pressure, R_a is airway resistance, L_a is the inertance of the gas in the airways, and C_g accounts for gas compressibility in the alveolar space. Similarly, the chest wall and muscle tissue impedances are represented by R_{ti}, L_{ti}, and C_{ti}. For the freely respiring animal, the breathing frequencies are low enough such that there are very minimal air or tissue mass momentum effects. That is, the impedances of the inductors L_{ti} and L_a are usually negligible (see, for example, Gomes et al., 2000).

In later models, the lung tissue parameters, R_{ti} and C_{ti}, have been shown to be frequency dependent, and can be described by the constant phase model (Hantos et al., 1992) at low frequencies generated in the breathing pattern of a freely respiring animal. In the steady-state s-domain, the constant phase model describes a filter of the form:

$$Z_{ti}(s) = \frac{Q}{s^{\alpha}} \tag{1}$$

where Z_{ti} is tissue impedance. This model can also be written in the Fourier (frequency) domain as:

$$Z_{ti}(\omega) = \frac{G - jH}{\omega^{\alpha}} \tag{2}$$

where G represents tissue damping (reflecting energy dissipation) and H is a parameter closely related to tissue elastance (reflecting energy conservation). The fractional exponent α can be written in terms of G and H as follows:

$$\alpha = \left(\frac{2}{\pi}\right) arctan\left(\frac{H}{G}\right). \tag{3}$$

Additionally, if the relationship between the real and imaginary parts of Eq. (2) is equated to the impedance of a series combination of R_{ti} and C_{ti}, it can be shown that:

$$R_{ti} = \frac{G}{\omega^{\alpha}} \tag{4}$$

and

$$C_{ti} = \frac{1}{H\omega^{1-\alpha}}. \tag{5}$$

Models like the one in Fig. 2 were developed for systems where a driving pressure was induced at either the thorax or the airway opening. In these types of applications, spontaneous respiration is a confounding factor. In humans, this is often dealt with by having the subject hold their breath. When dealing with animals, the animal is either anesthetized and paralyzed and kept on a ventilator which is temporarily stopped during the test, or the driving signal is designed such that the breathing frequencies do not interfere with the test. In any case, these models assume I_t and I_{ao} are due to the driving oscillations, not spontaneous respiration.

In the model presented in Fig. 3, an ideal pressure source represents the pressure, P_m, developed internally by the muscles to produce spontaneous respiration. When pressure is applied at the thorax or at the airway opening, the pressure P_m is added to the driving pressure. Note that the current, I_t, can be measured, while the pressure P_m is a generalized internal pressure source.

As the warmed humidified gas leaves the respiratory system, it cools as it mixes with the ambient air. There is evidence that this cooling process has a significant time constant associated with it (i.e., it is not instantaneous) in humans (Peslin et al., 1995, 1976). Tests in

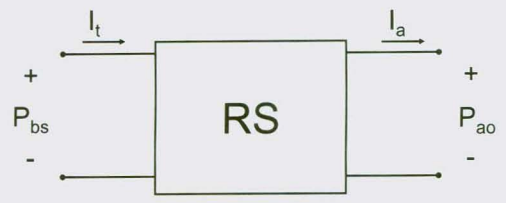

Fig. 1. Simple input–output model of the respiratory system.

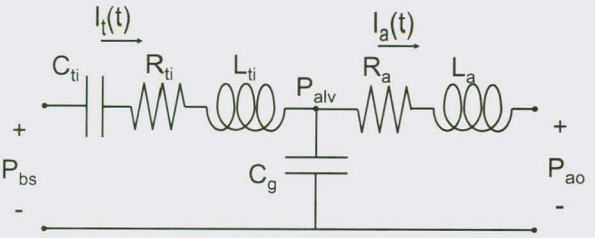

Fig. 2. Dubois respiratory model.

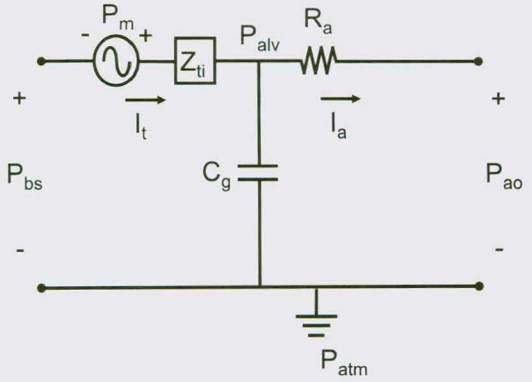

Fig. 3. Respiratory model of a freely respiring animal.

our laboratory indicate that this effect is nearly instantaneous in rats, and presumably in smaller animals such as the mouse. Schmid (1975) studied the exit temperature of respired air for many small mammals, including several species of mice, and found that, due to design of the nasal cavity, the exit temperature is approximately 1 °C above ambient.

On inspiration, the reverse takes place. That is, the ambient gas expands as it is warmed and humidified. When the thermal effect is instantaneous, it simply acts as a gain, G_t, on the airway flow. The value of G_t (Drorbaugh & Fenn, 1955; Peslin et al., 1995) is:

$$G_t = 1 - \frac{T_i}{T_a}\left[\frac{P_a - P_{H_2O_a}}{P_i - P_{H_2O_i}}\right] \tag{6}$$

where the subscripts i and a denote conditions of inspired and alveolar gas, respectively, and T and P are temperature and pressure, respectively. This effect can be modeled using a dependent current source as shown in Fig. 4. The current I_{ao} represents the current at the airway opening at atmospheric conditions.

Summing the currents at the two nodes in Fig. 4 gives:

$$I_{ao}(t) = I_a(t) - G_t I_a(t) = (1 - G_t) I_a(t) \tag{7}$$

and

$$I_t(t) = I_c(t) + I_a(t) \tag{8}$$

where $I_c(t)$ is the current through C_g and is given by

$$I_c(t) = C_g \frac{dP_{alv}(t)}{dt}. \tag{9}$$

Alveolar pressure is

$$P_{alv}(t) = I_a(t)\, R_a + P_{ao}(t). \tag{10}$$

For an animal respiring outside of a plethysmograph (short circuit), or in a plethysmograph with a properly designed impedance, $P_{alv}(t) \gg P_{ao}(t)$ such that

$$P_{alv}(t) \approx I_a(t) R_a. \tag{11}$$

Substituting Eqs. (9) and (11) into Eq. (8)

$$I_t(t) = R_a C_g \frac{dI_a(t)}{dt} + I_a(t). \tag{12}$$

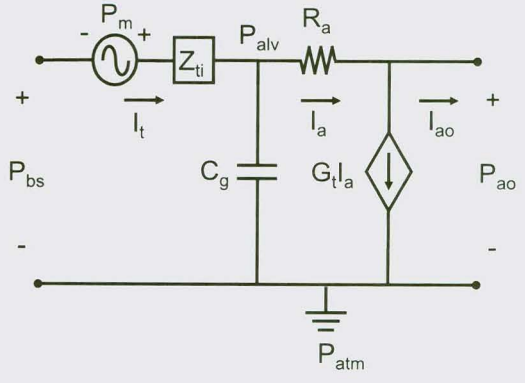

Fig. 4. Respiratory model of a freely respiring animal with temperature and humidity effects.

Taking the Laplace transform

$$I_t(s) = \left(R_a C_g s + 1\right) I_a(s) \tag{13}$$

$$\frac{I_a(s)}{I_t(s)} = \frac{1}{R_a C_g s + 1}. \tag{14}$$

Substituting Eq. (7) gives the transfer function:

$$\frac{I_{ao}(s)}{I_t(s)} = \frac{1 - G_t}{R_a C_g s + 1}. \tag{15}$$

Again, we note that the pressure, P_m cannot be measured, while thoracic flow, I_t often can be. Eqs. (14) and (15) provide a basis for analyzing a spontaneously breathing animal in a variety of systems in the following sections.

2.1. Specific airway resistance

In many pulmonary function screening situations, there is a desire to measure airway resistance, R_a. With most current noninvasive techniques, one cannot measure R_a alone. It is possible, however, to measure the product $R_a C_g$. The compliance of the gas in the lung is defined as:

$$C_g \equiv \frac{V_{tg}}{P_B - P_{H_2O_a}} \tag{16}$$

where V_{tg} is thoracic gas volume. This gives:

$$R_a C_g = R_a \frac{V_{tg}}{P_B - P_{H_2O_a}}. \tag{17}$$

Since $P_B - P_{H_2O_a}$ is known (can be measured), it can be removed from the right hand side above by multiplication. The result is known as specific airway resistance, *sRaw*.

$$sRaw = R_a V_{tg} = R_a C_g \left(P_B - P_{H_2O_a}\right). \tag{18}$$

For measurements made over a relatively short span of time, the pressure term $P_B - P_{H_2O_a}$ can be considered a constant which relates $R_a C_g$ directly to specific airway resistance.

2.2. Open versus closed chamber impedance

In general, the impedance, Z_c, of a chamber can be described with a parallel combination of a resistor and a capacitor. The resistor, R_c, represents the viscous resistance of airflow from the chamber to the outside environment, and the capacitor, C_c, represents the compliance of the gas in the chamber. The general expression for chamber impedance is:

$$Z_c = \frac{R_c}{R_c C_c s + 1}. \tag{19}$$

In a closed box, where $R_c \to \infty$, the expression in Eq. (19) reduces to:

$$Z_c = \frac{1}{C_c s}. \tag{20}$$

The pressure measured across this impedance is $P = I Z_c$. Because of the integral term ($1/s$), the pressure is proportional to changes in volume.

In an open box, or semi-open box, the chamber is often designed such that the R_cC_cs term in the denominator is much less than one. In this case, the chamber impedance can approximated as:

$$Z_c \approx R_c. \tag{21}$$

This is usually true at low frequencies and when the impedance presented by C_c is much larger than R_c because the majority of the flow is shunted through R_c. This being the case, the pressure measured in the box is proportional to box flow.

Note that systems that supply fresh air to an animal in a box use a bias flow supplied through a very high impedance so that the chamber impedance is largely unaffected. Also, with proper calibration and compensation, flow or volume can be measured with either type of chamber. For an in-depth discussion of the advantages, disadvantages, and signal handling techniques of each type, see for example (Bates et al., 1996; Butler et al., 1986; Peslin & Fredberg, 1986; Stocks et al., 1996). In this review, we simply assume the box is optimally designed so that when the pressure is measured across a known impedance, the flow signal is accurately calculated.

3. Double chamber plethysmography

Using the double chamber plethysmograph (DCP), an animal is placed in a chamber in which a neck or nose seal separates the flow produced by external volume changes at the thorax and flow from the nares. Each chamber presents an impedance between the animal and the atmosphere as indicated in Fig. 5. The pressure across each chamber impedance can be measured and related to airflow. The transfer function between thoracic flow and head chamber flow is described by Eq. (15) and is illustrated in Fig. 6.

3.1. Tidal volume

Tidal volume can be measured directly from the head chamber flow and estimated from the thorax flow signal. Tidal volume is typically given in terms of body temperature pressure saturated (BTPS) conditions. By definition, the tidal volume signal can be written as a function of time as:

$$V_a(t) = \int I_a(t)\, dt. \tag{22}$$

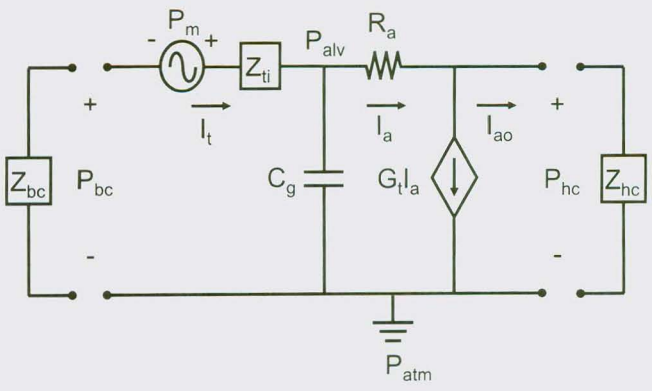

Fig. 5. Respiratory model of a freely respiring animal constrained in a double chamber plethysmograph.

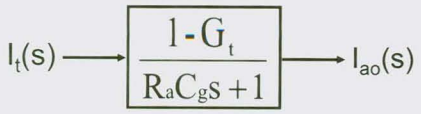

Fig. 6. Transfer function model of a freely respiring animal.

Using Eq. (7), the tidal volume can be calculated from the head chamber flow as:

$$V_a(t) = \frac{1}{1-G_t}\int I_{ao}(t)dt. \tag{23}$$

It should be noted that tidal volume is sometimes defined in terms of the change in volume of the thorax:

$$V_t(t) = \int I_t(t)\, dt. \tag{24}$$

The difference between $V_t(t)$ and $V_a(t)$ can be expressed in terms of the filter described by Eq. (14). At the limits as $R_aC_g\omega$ approaches zero, $V_a(t) = V_t(t)$, but as $R_aC_g\omega$ approaches infinity then $V_a(t) = 0$. Over most physiologically relevant ranges of R_aC_g and ω, there will be a phase shift between $V_a(t)$ and $V_t(t)$, but peak-to-peak amplitude (static tidal volume) differences are small under normal conditions.

3.2. Specific airway resistance

In the most common implementation of the double chamber plethysmograph, the phase shift of the transfer function shown in Fig. 6 is utilized to measure *sRaw* (R_aC_g).

After reaching steady state $s = j\omega$, and the phase shift θ of the transfer function is:

$$tan\ \theta = R_aC_g\omega. \tag{25}$$

If the breathing signal is considered sinusoidal, the specific airway resistance can be estimated from the phase shift at the fundamental breathing frequency (Pennock et al., 1979), f_{br}:

$$R_aC_g = \frac{tan(\theta)}{\omega} = \frac{tan(\theta)}{2\pi f_{br}}. \tag{26}$$

3.3. Pros/cons

The main advantage of the DCP is that specific airway resistance can be measured directly. Additionally, the pressure signals associated with these measurements are appreciable and are not as susceptible to measurement noise as compared with some other types of plethysmography. The flow signals measured in the DCP allow direct computation of tidal volume. Finally, it is possible to configure the DCP to enable the introduction of aerosols or gases into the head chamber for inhalation exposures. By estimating tidal volume from the thoracic flow, an estimate of the dose received by the animal can be acquired if the exposure concentration is known.

The main disadvantage of the DCP is related to the neck or nose seal since it is difficult to determine if the seal leaks. In addition, animal cooperation can be problematic. Animals can become agitated and may be difficult to position in the plethysmograph. The increased animal handling and physical constraint increases animal stress. Although the stress may not affect specific airway resistance, it certainly is capable of producing changes in respiratory rate and depth of breathing. Therefore, calculated values of tidal volume, respiratory rate, and minute ventilation using a DCP system may differ significantly from that of a calm, unrestrained animal. Obviously, the additional stress can also be a confounding factor when other biological markers are measured.

4. Head-out plethysmography

The head-out plethysmograph (HOP) is similar to the double chamber plethysmograph in that the head and body of the animal are separated in some manner by a seal. However, in the head-out plethysmograph, no provision is made to measure either pressure or airflow at the airway opening. Only the single measurement of thoracic flow is made using the HOP.

Now, consider the impedance seen by the pressure source P_m generated by the muscles of the thorax illustrated in Fig. 4. Since the impedance of the dependent current source, $G_t I_a$ is infinite, and the impedance presented by the compliance, C_g, of the gas in the lung airways is much larger than R_a, the model for the HOP can be approximated by that shown in Fig. 7a. When the breathing pattern is approximately sinusoidal, the model can be represented with fixed parameters as shown in Fig. 7b.

Using the general form for tissue impedance (see Eq. (1)) the system model corresponding to this circuit is shown in Fig. 8.

4.1. Tidal volume

Tidal volume measurements from the HOP are identical to those made from the body chamber of the DCP. That is, tidal volume is taken as the integral of thoracic flow (Eq. (24)).

4.2. Mid-expiratory flow

The most common parameter reported using the HOP is mid-expiratory flow (EF_{50}). A decrease in EF_{50} has been reported as an indicator of airway hyperresponsiveness (AHR) and bronchoconstriction in the mouse (Glaab et al., 2001; Neuhaus-Steinmetz et al., 2000; Vijayaraghavan et al., 1993) and in the rat (Glaab et al., 2002). Calculation of EF_{50} (illustrated in Fig. 9) is performed by first calculating tidal thoracic volume, $V_t(t)$ by integrating the flow signal, $I_t(t)$. The peak-to-peak volume excursion gives the thoracic tidal volume, V_T. Next, the flow during the expiratory phase corresponding to the midpoint of V_T yields the parameter EF_{50}. Analyzing the circuit in Fig. 7:

$$P_m(t) = \frac{1}{C_{ti}} \int I_t(t)\, dt + (R_a + R_{ti}) I_t(t). \tag{27}$$

When the inspiratory and expiratory volumes are equal, then the midpoint of V_T occurs when:

$$V_t(t) = \int I_t(t)\, dt = 0. \tag{28}$$

Then Eq. (27) reduces to

$$P_m = (R_a + R_{ti}) EF_{50}. \tag{29}$$

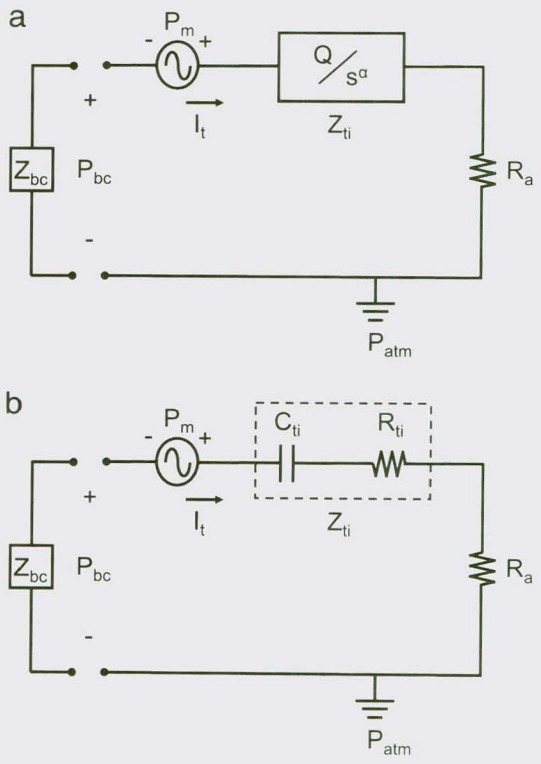

Fig. 7. (a) Respiratory model of a freely respiring animal in a head-out plethysmograph. (b) Single frequency model of a freely respiring animal in a head-out plethysmograph.

Fig. 8. Transfer admittance model of a freely respiring animal in a head-out plethysmograph.

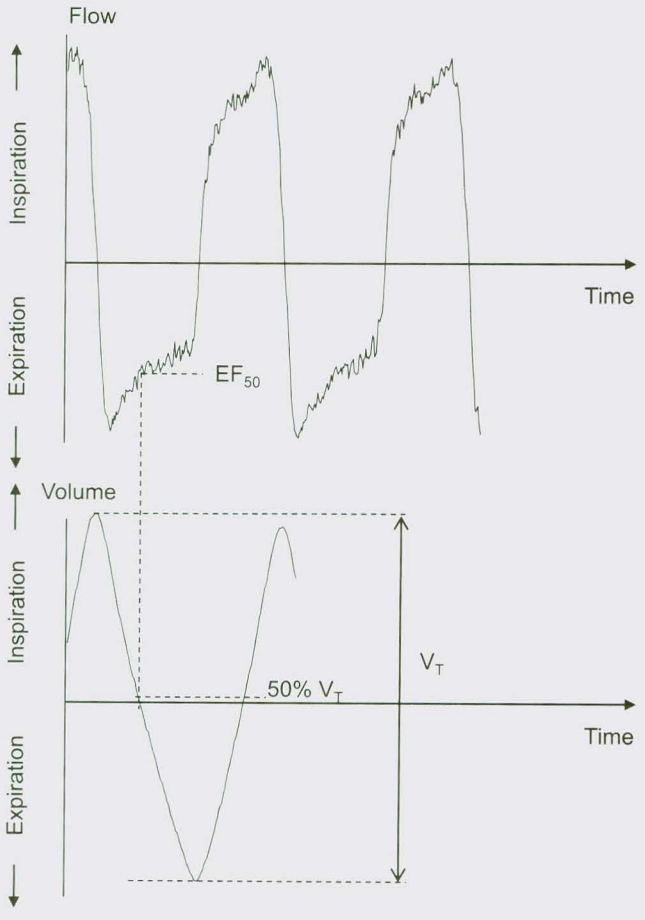

Fig. 9. Illustration of the calculation of EF_{50}.

Rearranging:

$$EF_{50} = \frac{P_m}{(R_a + R_{ti})}. \tag{30}$$

If it is assumed that $P_m(t)$ remains constant when $V_t(t) = 0$, then EF_{50} would be inversely proportional to pulmonary resistance ($R_L = R_{ti} + R_a$).

4.3. Pros/cons

The HOP shares most of the advantages of the DCP. Although it does not provide a direct measure of *sRaw*, it can be used to measure the EF_{50} parameter. Additionally, since no efforts need be made for measuring flow in the head chamber, this system should be slightly easier to use compared with the DCP method while exposing animals in a plethysmograph.

The HOP shares the same disadvantages with the DCP with respect to the integrity of the neck seal. Another disadvantage of the HOP is related to the parameter EF_{50}. Although EF_{50} has been shown to correlate with measurements of lung impedance under some experimental conditions, the single measurement of flow in the HOP is not sufficient to make a quantitative estimate of pulmonary impedance. As pointed out previously, one must assume that the internal driving pressure generated by the animal remains constant when $V_t = 50\%V_T$. It remains unclear how well these conditions are met. Even when the above assumption is met, however, according to the model of Eq. (30), a change in frequency would produce a change in EF_{50} since tissue resistance is frequency dependent (see Eq. (4)). This implies that EF_{50} could change without a change in the underlying tissue properties, damping (G), and elastance (H).

5. Whole-body plethysmography

Unlike the previously mentioned systems, an animal in the whole-body plethysmograph (WBP) has no restraints and no seal to separate the interactions between thoracic and nasal flows. A representation of this interaction is shown in Fig. 10. Flow into the WBP is:

$$I_b(t) = I_t(t) - I_{ao}(t). \tag{31}$$

Taking the Laplace transform of Eq. (31) and replacing $I_{ao}(s)$ with the expression given in Eq. (15) results in the following transfer function between $I_b(s)$ and $I_t(s)$:

$$\frac{I_b(s)}{I_t(s)} = \frac{RCs + G_t}{RCs + 1} = \frac{RCs}{RCs + 1} + \frac{G_t}{RCs + 1}. \tag{32}$$

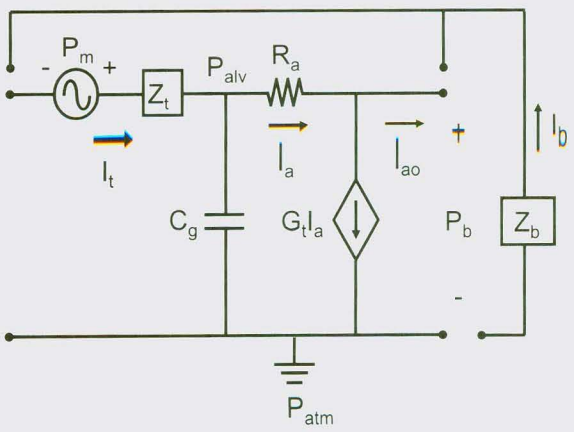

Fig. 10. Respiratory model of a freely respiring animal in a whole-body plethysmograph.

The system model is shown in Fig. 11.

At typical breathing frequencies

$$\frac{I_b(s)}{I_t(s)} \approx R_a C_g s + G_t \tag{33}$$

such that

$$I_b(s) \approx R_a C_g s I_t(s) + G_t I_t(s). \tag{34}$$

The first term on the right of Eq. (34) represents gas compression while the second represents gas conditioning effects.

5.1. Tidal volume

The WBP has been used to measure tidal volume (Drorbaugh & Fenn, 1955; Epstein & Epstein, 1978; Jacky, 1980). In those cases, the gas compression component of the signal was either ignored or assumed to be negligible. If the gas compression component is sufficiently small, which may the case for animals with normal lung function, the equation above reduces to:

$$I_b(s) = G_t(s) \tag{35}$$

and tidal volume can be written as:

$$V_t(t) = \frac{1}{G_t}\int I_b(t)\,dt. \tag{36}$$

5.2. Enhanced pause

The other measurement commonly made with the WBP is the enhanced pause parameter, or *Penh* (Hamelmann et al., 1997).

Penh is a dimensionless parameter defined as:

$$Penh = \frac{PEF}{PIF}\left[\frac{T_e - T_r}{T_r}\right] \tag{37}$$

where *PEF* is peak expiratory flow, *PIF* is peak inspiratory flow, T_e is expiratory time, and T_r is relaxation time, defined as the time to reach 64% of expiratory volume (see Fig. 12). Note that the flows in this equation represent the expiratory and inspiratory portions of box flow, I_b.

Penh of the airflow pattern into and out of the WBP has been shown to correlate with changes in lung resistance and dynamic lung compliance in response to methacholine (Hamelmann et al., 1997) and has been used by numerous investigators in studies of airway responsiveness or for long-term (hours and days) measurement of changes in pulmonary function. As an empirically-derived shape index, it is difficult to relate *Penh* directly to the system model shown in Fig. 11. However, Frazer et al. (2011) have recently shown that in some circumstances, changes in *Penh* can be related to changes in *sRaw* based on the shape of the thoracic flow pattern, I_t. The interpretation of *Penh* measurements has proven to be controversial, and many investigators have shown that changes in *Penh* do not always correlate with changes in lung mechanics.

Adding to the controversy is that there appears to be some discrepancies in the analysis of *Penh*. In the original research, *Penh* was applied to the pressure signal produced by an animal in a semi-open

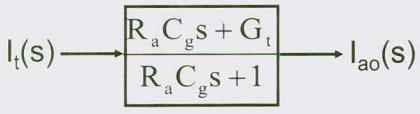

Fig. 11. Transfer function model of a freely respiring animal in a whole-body plethysmograph.

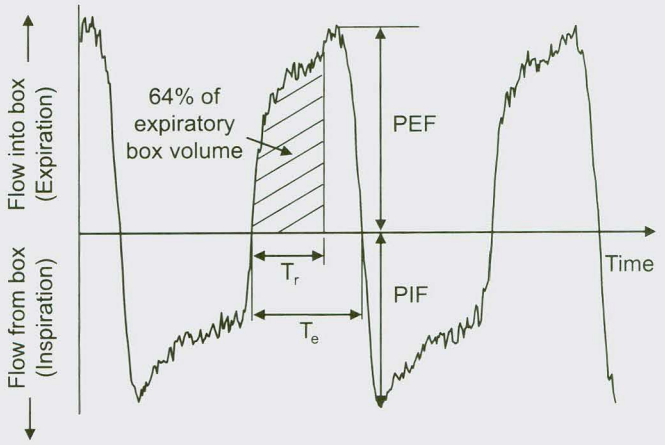

Fig. 12. Illustration of parameters for calculating *Penh*.

WBP, where the pressure signal is proportional to flow into and out of the box (see Section 2.2). This is the reason that *Penh* has been defined in this review in terms of the WBP flow signal. However, it has been pointed out (Lomask, 2006) that some have analyzed *Penh* in terms of the signal from a closed WBP, where the pressure signal is proportional to the integral of the box flow(see Section 2.2). Because the integral is a smoothing function, *Penh* does not respond to the volume signal in the same way it does to the flow signal.

Other investigators have applied *Penh* to the thoracic flow signal (Flandre et al., 2003). It can be shown that *Penh* of the thoracic flow would normally be inversely related to *Penh* of the WBP box flow (Frazer et al., 2011).

5.3. Pros/cons

The main advantage of the WBP is that it is extremely simple to use. Of all the systems, the WBP requires the least technician interaction and is the least stressful on the animal. Because of this, if food and water are provided, the WBP can allow long-term monitoring of the animals.

The main disadvantage of the WBP is that the signal acquired from the system is difficult to interpret. From Eq. (34), it can be seen that the box flow measured using a WBP is a function of gas conditioning, specific airway resistance, and the thoracic flow. As demonstrated in the section on the HOP, thoracic flow is a function of the driving pressure, tissue impedance, and airway resistance. So there are a number of factors that combine to determine the shape of the WBP signal. Because of this, a number of investigators have questioned the validity of the *Penh* measurement (Adler et al., 2004; Drazen et al., 1999; Enhorning et al., 1998; Lundblad et al., 2002; Mitzner & Tankersley, 2003; Sly et al., 2005).

6. Restrained whole-body plethysmography

The restrained whole-body plethysmograph (RWBP) (Agrawal, 1981; Lofgren et al., 2006) is basically a DCP contained within a traditional WBP. In this system, the animal is restrained such that airflow from the airway opening is measured with a heated pneumotach.

6.1. Tidal volume

Tidal volume measurements in the RWBP are taken directly from the flow measured with the pneumotach:

$$V_a(t) = \int I_a(t)\,dt. \tag{38}$$

6.2. Specific airway resistance

After passing through the pneumotach, the air interacts with the air in the chamber as in the WBP. Substituting Eq. (13) into Eq. (32):

$$I_b(s) = \left(R_a C_g s + G_t\right) I_a(s). \tag{39}$$

Although the data could be fitted to the equation above, a different strategy has been applied in the past (Agrawal, 1981). It is assumed that G_t is minimized during the transition from expiration to inspiration. If $G_t = 0$, then Eq. (39) reduces to:

$$I_b(s) = I_a(s)\, R_a C_g s \tag{40}$$

or

$$\frac{I_b(s)}{s} = I_a(s)\, R_a C_g \tag{41}$$

$$V_b(s) = I_a(s)\, R_a C_g. \tag{42}$$

In the time domain

$$V_b(t) = I_a(t)\, R_a C_g. \tag{43}$$

Therefore, specific airway resistance can be estimated from the slope of a plot of box volume versus airway flow during the segments of time when G_t is minimized (i.e., airflow during the transition from expiration to inspiration (Agrawal, 1981)).

6.3. Pros/cons

This plethysmograph provides an alternative to the traditional double chamber plethysmograph. Because this system is essentially a restrained plethysmograph with a neck or nose seal, this plethysmograph shares the same advantages and disadvantages as the DCP.

7. Video-assisted plethysmography

The video-assisted plethysmograph (VAWBP) (Bates et al., 2008) is essentially a whole-body plethysmograph that estimates the change in volume of the thorax using video cameras.

7.1. Tidal volume

In this system, two cameras provide images of the silhouette of an animal from orthogonal angles. Volume is inferred from these silhouette images assuming the mouse has an elliptical cross-section.

7.2. Specific airway resistance

Several groups of pulmonary physiologists have shown derivations of the relationship between thoracic volume change, the WBP pressure signal, and airway resistance (Bates et al., 2008; Lai-Fook & Lai, 2005; Lundblad et al., 2002). An alternate derivation can be illustrated starting with Eq. (32).

$$\frac{I_b(s)}{I_t(s)} = \frac{R_a C_g s + G_t}{R_a C_g s + 1}.$$

At low frequencies, Eq. (32) reduces to:

$$\frac{I_b(s)}{I_t(s)} \approx R_a C_g s + G_t. \tag{44}$$

In the VAWBP, the plethysmograph interior is heated and humidified to minimize the effects of G_t. As G_t approaches zero:

$$\frac{I_b(s)}{I_t(s)} = R_a C_g s. \tag{45}$$

Since, the impedance of a closed chamber is

$$Z_b(s) = \frac{1}{C_b s} = \frac{P_b(s)}{I_b(s)}. \tag{46}$$

This results in the following expression:

$$I_b(s) = P_b(s)\, C_b s. \tag{47}$$

Combining Eqs. (45) and (47) gives:

$$\frac{P_b(s)\, C_b s}{I_t(s)} = R_a C_g s \tag{48}$$

or

$$P_b(s) = \frac{R_a C_g}{C_b} I_t(s). \tag{49}$$

Since compliance is volume divided by pressure

$$P_b(s) = \frac{R_a V_{tg}}{V_{box}} I_t(s) \tag{50}$$

or

$$P_b(s) = \frac{sRaw}{V_{box}} I_t(s). \tag{51}$$

Integrating both sides gives:

$$\frac{P_b(s)}{s} = \frac{sRaw}{V_{box}} V_t(s). \tag{52}$$

This can be written in the time domain as:

$$\int P_b(t)\, dt = \frac{sRaw}{V_{box}} V_t(t) \tag{53}$$

which is coincident with the expressions derived by Lundblad et al. (2002), Lai-Fook and Lai (2005) and Bates et al. (2008). *sRaw* can then be determined by fitting the data measured by the VAWBP to the equation above (Bates et al., 2008).

7.3. Pros/cons

The obvious advantage of video-assisted plethysmograph is that it can provide a direct measure of specific airway resistance in an unrestrained, freely respiring mouse. The disadvantages of this system include a somewhat slow (25 Hz) sampling resolution (presumably from the camera speed and/or the image processing speed), and the fact that animal motion would appear to be problematic. Additionally, the authors of this technique chose to heat and humidify the system. While this has the advantage of eliminating the thermohygrometric gain from the model, it does make the system somewhat more complicated. Additionally, it is not clear what stresses the heat may place on the animal in the system. However, it seems possible that this system could be implemented by modeling the heat/humidity effect as described by Peslin and Duvivier (1999).

8. X-ray plethysmography

Lai-Fook et al. (2008) have used x-rays to complement a traditional WBP. This system is similar to the VAWBP in that it utilizes a closed chamber and conditioned gas to mitigate the effects of temperature and humidity. Bates et al. (2008) have pointed out some practical limitations of the x-ray method, including the fact that this system cannot collect images rapidly throughout a breath, and that image segmentation has to be performed manually. These limitations, and perhaps the cost of the x-ray system itself, make this method an unlikely candidate as a screening tool. An advantage of this system, however, is the ability to estimate thoracic gas volume, allowing separate measurements of R_a and C_g.

9. Acoustic plethysmography

Acoustics have been used to measure tidal volume in mice (Reynolds & Frazer, 2006) and in neonatal mice (Daubenspeck et al., 2008). In these whole-body systems, the plethysmograph impedance, Z_b, is minimized in order to maximize the fidelity of the thoracic volume measurement. Reynolds et al. (2008) later extended the acoustic plethysmograph so that both thoracic volume and plethysmograph flow could be measured, allowing an estimate of specific airway resistance.

9.1. Tidal volume

This system sets up the whole-body plethysmograph as a resonant cavity so that changes in the volume of the animal produce a modulation of the sound amplitude within the chamber. The acoustic excitation frequency is much higher than the breathing frequency, and the demodulated signal provides a direct measure of the tidal volume as a function of time.

9.2. Specific airway resistance

Similar to methods utilized with the DCP, the acoustic plethysmograph estimates *sRaw* from the phase angle between thoracic flow and box flow. This is shown by rewriting Eq. (32):

$$\frac{I_b(s)}{I_t(s)} = \frac{R_a C_g s + G_t}{R_a C_g s + 1}$$

where the phase angle, θ, between thoracic flow and box flow is given by

$$tan\,\theta = \frac{(1-G_t)\,\omega R_a C_g}{G_t + \omega^2 R_a^2 C_g^2}. \tag{54}$$

Rearranging Eq. (54) gives:

$$\omega^2\, tan\,\theta \left(R_a C_g\right)^2 - \omega(1-G_t)\, R_a C_g + G_t\, tan\,\theta = 0. \tag{55}$$

The higher order term is small over physiologically-relevant ranges and can be ignored. Solving for $R_a C_g$ results in the following solution

$$R_a C_g = \frac{G_t\, tan\,\theta}{2\pi(1-G_t)f}. \tag{56}$$

9.3. Pros/cons

Like the VAWBP, the advantage of the acoustic plethysmograph is that it provides a direct measurement of specific airway resistance in an unrestrained, freely respiring animal. A disadvantage of the system is the fact that it is susceptible to noise induced from ambient noise

frequencies near the excitation frequency. Additionally, while the acoustic excitation is outside the hearing range of the mouse, it is not known if the vibration produced by the acoustic resonance places any additional stresses on the animal.

10. Discussion

Several techniques commonly used for pulmonary function screening have been reviewed here using a simple mathematical and electrical equivalent model of the respiratory system as a basis. While we believe the models presented are generally appropriate, there are some drawbacks. First, these models assume the lung behaves as a linear system that can be described by lumped parameter impedances. While this may be reasonable for animals with normal to moderately-diseased lung function, it may not be accurate under severe respiratory conditions. Similarly, a model of the lung assuming a single airway connected to a single air space is likely to be inaccurate under severe conditions.

Additionally, many parameters of these models are assumed to be constant even though they have some variance with respect to volume or flow. For instance, the impedance of thoracic gas is described by a constant compliance, C_g, ignoring the fact that it varies with the change in lung volume during respiration. Likewise, the thermohygrometric gain, G_t, likely has some variance between inspiration and expiration (Epstein & Epstein, 1978; Lomask, 2006; Mitzner & Tankersley, 2003; Reynolds et al., 2008), but is assumed symmetric in the models presented here.

It should be emphasized that the focus of this review is noninvasive pulmonary function testing. While noninvasive methods have many advantages that have already been discussed (i.e., repeatability in the same animal, natural conditions, etc.), there are also limitations. Notably, they lack the accuracy of conventional invasive methods where the frequency and amplitude of perturbations applied to the lung are precisely controlled. Additionally, invasive methods by-pass (via tracheostomy) the upper airways, whose mechanical properties must certainly be included in any noninvasive measurement.

Each of the systems that have been reviewed can be classified as either restrained or unrestrained, and as a one- or two-measurement system. In general, the systems that restrain the animal to make measurements tend to be more difficult to use and likely produce more stress than unrestrained systems. On the other hand, restrained systems tend to produce higher-level signals and are less prone to motion-induced or environmental noise. The one-measurement systems tend to be easier to implement and use than the two-measurement systems, but sometimes unwarranted assumptions are necessary to relate the derived parameters to lung mechanics. In contrast, two-measurement systems make it possible for the direct determination of specific airway resistance. With respect to this issue, it is important to note that none of these systems provides a direct measure of lung tissue impedance, which can only be directly determined by invasive means.

In summary, we have reviewed several methods for pulmonary function screening in small laboratory rodents. It has been shown how each of these systems interfaces to a common pulmonary model of a freely respiring animal, providing a unified approach to the many manifestations of noninvasive lung mechanics measurement. It is our hope that the analysis presented here elucidates relationships among methods and provides a reasonable basis for the appropriate choice of a screening tool and the interpretation of the results.

Disclaimer

The findings and conclusions in this report are those of the authors and do not necessarily represent the views of the National Institute for Occupational Safety and Health.

References

Adler, A., Cieslewicz, G., & Irvin, C. G. (2004). Unrestrained plethysmography is an unreliable measure of airway responsiveness in balb/c and c57bl/6 mice. *J Appl Physiol*, 286–292.

Agrawal, K. P. (1981). Specific airway conductance in guinea pigs: Normal values and histamine induced fall. *Respir Physiol*, 23–30.

Bates, J., & Irvin, C. (2003). Measuring lung function in mice: The phenotyping uncertainty principle. *J Appl Physiol*, 1297–1306.

Bates, J. H. T., Thompson-Figueroa, J., Lundblad, L. K. A., & Irvin, C. G. (2008). Unrestrained video-assisted plethysmography: A noninvasive method for assessment of lung mechanical function in small animals. *J Appl Physiol*, 253–261.

Bates, J. H. T., Turner, M. J., Lanteri, C. J., Jonson, B., & Sly, P. D. (1996). Measurement of flow and volume. In J. Stock, P. D. Sly, R. S. Tepper, & W. J. Morgan (Eds.), *Infant respiratory function testing* (pp. 81–116). New York: Wiley-Liss, Inc.

Butler, J. P., Leith, D. E., & Jackson, A. C. (1986). Principles of measurement: Applications to pressure, volume, and flow. In A. P. Fishman, P. T. Maclem, J. Mead, & S. R. Geiger (Eds.), *Handbook of physiology, Section 3: The respiratory system, Volume III. Mechanics of breathing, Part I chapter 2* (pp. 15–33). Maryland: American Physiological Society.

Daubenspeck, J. A., Li, A., & Nattie, E. E. (2008). Acoustic plethysmography measures breathing in unrestrained neonatal mice. *J Appl Physiol*, 262–268.

Drazen, J. M., Finn, P. W., & De Sanctis, G. T. (1999). Mouse models of airway responsiveness: Physiological basis of observed outcomes and analysis of selected examples using these outcome indicators. *Annu Rev Physiol*, 593–625.

Drorbaugh, J. E., & Fenn, W. O. (1955). A barometric method for measuring ventilation in newborn infants. *Pediatrics 16*, 81–87.

DuBois, A. B., Brody, A. W., Lewis, D. H., & Burgess, B. F. J. (1956). Oscillation mechanics of lungs and chest in man. *J Appl Physiol*, 587–594.

Enhorning, G., van Schaik, S., Lundgren, C., & Vargas, I. (1998). Whole-body plethysmography, does it measure tidal volume in small animals. *Can J Physiol Pharmacol*, 945–951.

Epstein, M. A., & Epstein, R. A. (1978). A theoretical analysis of the barometric method for measurements of tidal volume. *Respir Physiol*, 105–120.

Flandre, T. D., Leroy, P. L., & Desmecht, D. J. M. (2003). Effect of somatic growth, strain, and sex on double-chamber plethysmographic respiratory function values in healthy mice. *J Appl Physiol*, 1129–1136.

Frazer, D. G., Reynolds, J. S., & Jackson, M. C. (2011). Determining when enhanced pause (penh) is sensitive to changes in specific airway resistance. *J Toxicol Env Heal A*, 287–295.

Glaab, T., Daser, A., Braun, A., Neuhaus-Steinmetz, U., Fabel, H., Alarie, Y., et al. (2001). Tidal midexpiratory flow as a measure of airway hyperresponsiveness in allergic mice. *Am J Physiol Lung Cell Mol Physiol*, L565–L573.

Glaab, T., Hoymann, H. G., Hohlfeld, J. M., Korolewitz, R., Hecht, M., Alarie, Y., et al. (2002). Noninvasive measurement of midexpiratory flow indicates bronchoconstriction in allergic rats. *J Appl Physiol*, 1208–1214.

Glaab, T., Taube, C., Braun, A., & Mitzner, W. (2007). Invasive and noninvasive methods for studying pulmonary function in mice. *Respir Res*, 63.

Glaab, T., Ziegert, M., Baelder, R., Korolewitz, R., Braun, A., Hohlfeld, J. M., et al. (2005). Invasive versus noninvasive measurement of allergic and cholinergic airway responsiveness in mice. *Respir Res*, 139.

Gomes, R. F. M., Shen, X., Ramchandani, R., Tepper, R. S., & Bates, J. H. T. (2000). Comparative respiratory system mechanics in rodents. *J Appl Physiol*, 908–916.

Hamelmann, E., Schwarze, J., Takeda, K., Oshiba, A., Larsen, G. L., Irvin, C. G., et al. (1997). Noninvasive measurement of airway responsiveness in allergic mice using barometric plethysmography. *Am J Respir Crit Care Med*, 766–775.

Hantos, Z., Daroczy, B., Suki, B., Nagy, S., & Fredberg, J. J. (1992). Input impedance and peripheral inhomogeneity of dog lungs. *J Appl Physol*, 168–178.

Hoymann, H. (2006). Invasive and noninvasive lung function measurements in rodents. *J Pharmacol Toxicol*, 16–26.

Jacky, J. P. (1980). Barometric measurement of tidal volumes: Effects of pattern and nasal temperature. *J Appl Physiol*, 319–325.

Lai-Fook, S. J., Houtz, P. K., & Lai, Y. (2008). End-expiratory and tidal volumes measured in conscious mice using single projection x-ray images. *J Appl Physiol*, 521–533.

Lai-Fook, S. J., & Lai, Y. (2005). Airway resistance due to alveolar gas compression measured by barometric plethysmography in mice. *J Appl Physiol*, 2204–2218.

Lofgren, L. S., Mazan, M. R., Ingenito, E. P., Lascola, K., Seavey, M., Walsh, A., et al. (2006). Restrained whole body plethysmography for measure of strain-specific and allergen induced airway responsiveness in conscious mice. *J Appl Physiol*, 1495–1505.

Lomask, M. (2006). Further exploration of the penh parameter. *Exp Toxicol Pathol*, 13–20.

Lundblad, L. K. A., Irvin, C. G., Adler, A., & Bates, J. H. T. (2002). A reevaluation of the validity of unrestrained plethysmography in mice. *J Appl Physiol*, 1198–1207.

Mitzner, W., & Tankersley, C. (2003). Interpreting penh in mice. *J Appl Physiol*, 828–832.

Neuhaus-Steinmetz, U., Glaab, T., Daser, A., Braun, A., Lommatzsch, M., Herz, U., et al. (2000). Sequential development of airway hyperresponsiveness and acute airway obstruction in a mouse model of allergic inflammation. *Int Arch Allergy Immunol*, 57–67.

Pennock, B. E., Cox, C. P., Rogers, R. M., Cain, W. A., & Wells, J. H. (1979). A noninvasive technique for measurement of changes in specific airway resistance. *J Appl Physiol*, 399–406.

Peslin, R., & Duvivier (1999). Removal of thermal artifact in alveolar pressure measurement during forced oscillation. *Respir Physiol*, 141–150.

Peslin, R., Duvivier, C., Vassiliou, M., & Gallina, C. (1995). Thermal artifacts in plethysmographic airway resistance measurements. *J Appl Physiol*, 1958–1965.

Peslin, R., & Fredberg, J. J. (1986). Oscillation mechanics of the respiratory system. In A. P. Fishman, P. T. Maclem, J. Mead, & S. R. Geiger (Eds.), *Handbook of Physiology, Section 3:*

The Respiratory System, Volume III. Mechanics of Breathing, Part I (pp. 15–33). Maryland: American Physiological Society chapter 11.

Peslin, R., Jardin, P., & Hannhart, B. (1976). Modeling of the relationship between volume variations at the mouth and chest. *J Appl Physiol*, 659–667.

Reynolds, J., & Frazer, D. (2006). Unrestrained acoustic plethysmograph for measuring tidal volume in mice. *Ann Biomed Eng*, 1494–1499.

Reynolds, J., Johnson, V., & Frazer, D. (2008). Unrestrained acoustic plethysmograph for measuring specific airway resistance in mice. *J Appl Physiol*, 711–717.

Schmid, W. (1975). Temperature gradients in the nasal passage of some small mammals. *Comp Biochem Physiol A*, 304–308.

Sly, P., Turner, D., Collins, R., & Hantos, Z. (2005). Penh is not a validated technique for measuring airway function in mice. *Am J Resp Crit Care Med*, 256.

Stocks, J., Marchal, F., Kraemer, R., Gutkowski, P., Yishay, E. B., & Godfrey, S. (1996). Plethysmographic assessment of functional residual capacity and airway resistance. In J. Stock, P. D. Sly, R. S. Tepper, & W. J. Morgan (Eds.), *Infant respiratory function testing* (pp. 191–239). New York: Wiley-Liss, Inc.

Vijayaraghavan, R., Schaper, M., Thompson, R., Stock, M., & Alerie, Y. (1993). Characteristic modifications of the breathing pattern of mice to evaluate the effects of airborne chemicals on the respiratory tract. *Arch Toxicol*, 478–490.